

# Deep Learning Technique for Detecting and Analysing Ischemic Stroke Using MRI Images

Noor Ayesha<sup>1\*</sup>, H S Sheshadri<sup>2</sup>

<sup>1\*,2</sup>Department of Electronics and Communications Engineering, P.E.S College of Engineering, Mandya, India

## Abstract

The quantitative analysis of cerebral MRI images plays a pivotal role in stroke diagnosis and treatment. Deep learning, particularly CNNs, with their robust learning capabilities, offer an effective tool for lesion detection. To address the unique properties of stroke injuries and automate detection processes, we compiled a dataset of brain MRI images from various medical sources, representing patients affected by ischemic strokes. Different deep learning-based networks, including “Single Shot Multibox Detector (SSD)”, “Region-based CNN with ResNet101 (RCNN-ResNet101)”, “RCNN with VGG16 (RCNN- VGG16)”, and “YOLOV3”, were employed for automated lesion detection. The evaluation focused on achieving optimal precision in comparison to existing methods across Diffused Weight, Flair, and T1 modalities of MRI datasets. The developed technique involves extracting deep features during the encoding stage, followed by the minimization of features using fully connected layers. Significant handcrafted features, such as Local Binary Pattern (LBP) and Gray Level Co-occurrence Matrix (GLCM), were incorporated alongside deep features. The concatenation of these features was implemented to maximize the dimension of the feature vector. This concatenated vector was then used to train and test the performance of various classifiers. Binary classification was employed to categorize brain images into normal or stroke affected. Initially, SoftMax was used as the default classifier. The performance of each classifier was individually evaluated, and the best-performing classifier was selected to confirm the overall effectiveness of the proposed technique. This all-encompassing strategy not only leverages deep learning for automatic lesion detection but also integrates handcrafted features and diverse classifiers to improve the precision and dependability of stroke detection across various brain MRI image modalities.

**Keywords**-Convolutional Neural Network, Deep Learning, Ischemic stroke, Magnetic Resonance Imaging, YOLOV3

## I. Introduction

Ischemic stroke is a prevalent and impactful medical condition that significantly affects the quality of human life. The timely identification of the location and extent of the infarct core is crucial for accurate medical diagnosis and intervention. However, current assessment methods face limitations such as patient compliance, contraindications, and the complexity and time-consuming nature of the assessments, particularly in critical situations [1]. While a standard head non-contrast CT scan is a fundamental assessment for suspected ischemic stroke patients, its efficacy in identifying acute infarct cores is hindered by the subtle contrast between normal brain tissue and early infarct tissue, often beyond the perceptual limits of the naked eye.

The advent of artificial intelligence (AI) has presented an opportunity to overcome these challenges [2]. AI-powered machines can accurately analyze each pixel in medical images, discerning differences that may escape human observation. In recent studies, researchers have employed deep learning (DL) and optimization strategies to extract information about acute infarct cores from non-contrast CT images. This approach harnesses the characteristic and

diagnostically valuable features within the images, providing a potential breakthrough in enhancing diagnostic accuracy.

Stroke stands as a leading cause of adult disability globally, affecting up to two-thirds of individuals with long haul disabilities. It is a pervasive and perilous cerebrovascular disease, characterized by a neurological attack that damages the brain and disrupts its functionalities [3]. The two primary categories of stroke are ischemic and hemorrhagic strokes. Ischemic strokes occur when blood flow is disrupted in one of the brain's vessels, leading to the formation of a clot that obstructs blood flow to certain tissue areas, causing impairment of vital functions. Transient ischemic attacks may occur with minimal severity [4]. On the other hand, hemorrhagic strokes happen when a brain vessel ruptures, causing blood to flow into surrounding tissues. Approximately eighty percent of strokes fall into the category of ischemic strokes, with the remaining belonging to hemorrhagic strokes [5]. The advancement of AI, particularly deep learning applications, holds promise in revolutionizing the identification and understanding of ischemic strokes, potentially leading to more effective

diagnostic and therapeutic strategies.

The identification and assessment of infarcted brain tissue play a crucial role in the effective management of acute ischemic strokes. Patients with extensive infarction at the baseline may not benefit significantly from thrombectomy or thrombolysis procedures [2]. Non-contrast-enhanced CT scans are widely employed for evaluating the extent of localized necrosis in patients with acute strokes. The Alberta Strokes Program Early CT Scores offer a semiquantitative method for assessing the degree of localized necrosis in non-contrast-enhanced CT images [6]. However, utilizing this approach requires a certain level of expertise, which may not be readily available in smaller hospitals or during non-standard hours [7].

In this research work, the focus is on MR image processing to facilitate the detection, segmentation, and classification of white matter hyperintensities (WMHs). Advanced mechanisms, particularly artificial intelligence (AI), are employed to enhance the efficiency of these tasks. By leveraging AI, the goal is to automate and improve the accuracy of identifying and categorizing WMHs, providing a more accessible and efficient solution for medical professionals.

The continuous advancements in MRI techniques have positioned MRI as a promising tool for elucidating brain structure and function. Over time, brain MR image resolution has significantly improved since the introduction of the initial MR imaging technology [8]. This progress has enabled the examination of physical structures in the brain, visual assessment of cranial nerves, and the investigation of abnormalities in the posterior fossa and spinal cord.

Moreover, MRI presents benefits compared to CT, demonstrating reduced susceptibility to image artifacts. Analysis of MR slices proves valuable across diverse applications, encompassing lesion detection and segmentation, tissue delineation, and other diagnostic pursuits [9]. The integration of AI in MR image processing

holds promise for streamlining and improving ischemic stroke assessments, thereby facilitating more precise and timely diagnoses.

According to researchers [10], the etiology of White Matter Hyperintensities (WMHs) is often attributed to either a demyelinating or ischemic nature due to the lack of pathological investigations. When WMHs are influenced by a vascular obstruction, they are categorized as ischemic. On the other hand, if there is inflammation leading to the destruction and loss of the myelin layer, compromising neural transmissions [11], the WMH is considered demyelinating. Such demyelinating WMHs are frequently associated with conditions like multiple sclerosis.

Ischemic WMHs typically result from a reduction or blockage in blood flow, leading to insufficient oxygen and nutrient supply to the affected white matter areas in the brain. This ischemic insult can result from conditions such as small vessel disease, atherosclerosis, or other vascular abnormalities. The identification and understanding of the underlying cause of WMHs are essential for effective diagnosis and treatment planning.

WMHs characterized by demyelination, inflammation, and myelin loss are frequently linked to autoimmune conditions such as multiple sclerosis. In multiple sclerosis, the immune system erroneously targets the protective myelin sheath enveloping nerve fibers, resulting in communication issues between the brain and the body. The demyelination process may present as hyperintensities in MR images, offering valuable insights into the progression of the disease.

It's important for healthcare professionals to distinguish between ischemic and demyelinating WMHs, as the underlying cause can guide appropriate treatment strategies and interventions. Advanced techniques, including artificial intelligence-based image processing, are increasingly being utilized to improve precision and effectiveness of identifying and classifying WMHs in neuroimaging studies.

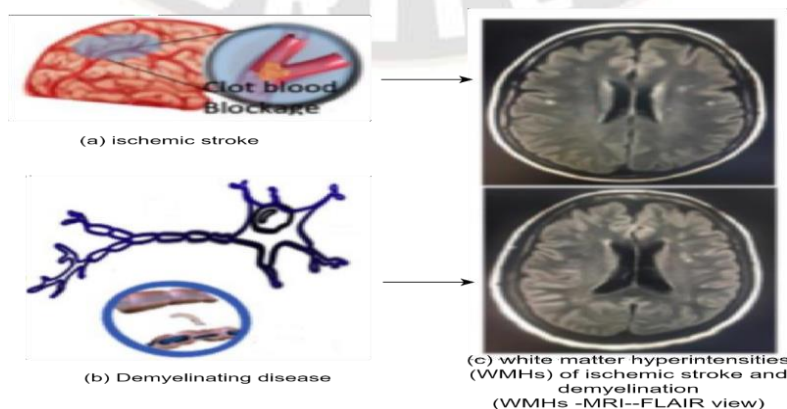


Fig.1: Considered diseases for research



## II. Related Works

A stroke occurs when the blood flow to a specific area of the brain is disrupted. According to the Bamford clinical classification system, there are three types of ischemic strokes [12]: (i) In this type, the anterior cerebral regions of the brain are affected. This can lead to various neurological symptoms and impairments depending on the specific location and extent of the ischemia. (ii) Lacunar strokes involve occlusions in vessels that supply blood to deep areas within the brain. These strokes can result in small, localized infarctions and are associated with specific clinical manifestations. (iii) In this category, large and severe strokes affect the anterior cerebral regions due to extensive ischemia. Total anterior circulation strokes can have a significant impact on brain function and may lead to severe neurological deficits [13]. Ischemic strokes are a common cerebrovascular disease [14] and a leading cause of death and disability, particularly in lower-income countries [15]. In more developed nations, approximately 75% of strokes are attributed to brain ischemia, where inadequate blood supply leads to damage in brain tissue. The remaining 15% of strokes are categorized as hemorrhagic strokes, where bleeding occurs within the brain [16].

The identification, detection, classification, and analysis of strokes heavily rely on medical imaging techniques such as CT scans and MRIs [17]. MRI enables the detection of smaller infarcts and provides a more accurate analysis of stroke lesions in both shallow and deep areas of the brain. This

heightened precision is because stroke areas are more clearly visible and delineated in MR slices compared to CT scans. The accurate delineation of the affected area is crucial for correct diagnosis, as strokes can be misinterpreted as other medical issues.

For identifying neurological disorders, including strokes and demyelinating diseases, manual segmentation and characterization of abnormal brain tissue are considered the gold standard for lesion recognition. However, this method is exceptionally tedious, relies on expert experience, and has its limitations. To address these challenges, automated detection of neurological issues becomes essential. Despite being a complex task due to data variability, such as the shape and location of ischemic stroke injuries, automated methods are crucial to handle the diversity in symptoms, affected sites, and patient differences [18].

The past few years have been an important time for research in the field of Artificial Intelligence (AI) and Deep Learning (DL) with a particular focus on automated or semi-automated tools, algorithms and methods for the detection of brain lesions such as tumors, strokes, gliomas, and etc [19][20][21]. A great deal of research indicates that deep

learning algorithms can help with different clinical tasks that involve image restoration, segmentation, pattern identification, diagnosis, and disease classification [22, 23]. In any case, it is a lot of hard work to develop a solid technique for the receivers to get an outcome as good as those of experts.

Table 1, list of terms and abbreviations related to articles on the management of ischemic stroke. These terms involve various strategies, procedures, and techniques used in the context of medical imaging and computer-assisted interventions. some of the key terms: **Strategies and Procedures:** SVM: Support Vector Machines, RF: Random Forest [24], WS: Watershed (segmentation technique) [25], DL: Deep Learning, CNNs: Convolutional Neural Networks [26][27], RF-SVM: Fusion of Random Forest and Support Vector Machines [28], RF-CNN: Fusion of Random Forest and Convolutional Neural Networks [29]. **Imaging Techniques:** DWI: The Diffusion-Weighted Imaging of MRI, PWI: The Perfusion-Weighted Imaging of MRI, FLAIR: The Fluid Attenuated Inversion Recovery of MRI. **Segmentation and Evaluation Metrics:** BRATS: Brain Tumor Image Segmentation, ISLES: Ischemic Stroke Lesion Segmentations, DSC: Dice Score Coefficients (an evaluation metric for proper segmentation), HD: Hausdorff Distance (a measure of the distance between two sets), ASSD: Average Symmetric Surface Distances. **Other Terms:** SPES: Stroke Perfusion Estimations, MICCAI: Medical Images Computing and Computer-Assisted Interventions, ANN: Artificial Neural Networks, RDF: Random Decision Forest, MUSCLE Net: Multi-Scale Convolutional Label Evaluations, EDD Net: Ensemble of Two Decon Nets.

CNN has achieved remarkable outcomes in computer vision. This aligns with the broader trend of CNN being highly effective in tasks such as image recognition, segmentation, and classification. CNN- dependent strategies have proven to be effective in segmenting ischemic stroke lesions on MRIs [35][36]. This involves pouring over countless fully annotated areas where stroke injuries have been meticulously labeled on a pixel-by-pixel basis. Demonstration in Figure 2 gives a few instances CNN- dependent strategies bring to the segmentation of ischemic stroke lesions. CNN, with their ability to learn hierarchical features from data, has shown substantial potential in handling complex tasks in medical image analysis. CNN typically has a large number of parameters (weights and biases), making them powerful but also resource-intensive. Additionally, the success of CNN-based strategies relies on having access to extensive datasets with fully annotated regions for training. The strategies based on CNN require significant amounts of fully annotated data to train the model effectively.

**Table 1.** Survey on central concepts in research, types of images utilized, and methodologies employed.

Disease	Type of Images/ Dataset	Methodology	Metrics/ Observation
Brain injuries; Ischemic stroke; Brain Tumours [30]	BRATS 2015; MRI; ISLES 2015	CNN; 11-layer deep; 3D;	<b>ISLES 2015</b> DSC: 66; Precisions: 77; ASSD: 5.00; Sensitivity: 63; Hausdorffs: 55.93 <b>BRATS 2015</b> Precision: 85.3; DSC: 84.9; Sensitivity: 87.7
Ischemic strokes [29]	MR_DWI_PWI	RF_CNN	Comparisons of algorithms built in Challenge ISLES 2015.
Ischemic strokes [18]	MRI: 40 patients	Generalized linear Models CNN, RDF	HD (mm): 15.79 DSC [0, 1]: 0.80 ASSD (mm): 2.03 Rec. [0, 1]: 0.911 Prec. [0, 1]: 0.73
Ischemic stroke [26]	MRDWI- 741 Private subjects	EDD Net CNN MUSCLE Decon Nets: Net	Lesion detection rate: 0.94 DSC: 0.67
Ischemic strokes [31]	ISLES2015 MRI-FLAIR-DWI	Optimization of social gathering moderated entropy of Fuzzy-Tsallis	DC: 88.54% Precisions: 98.11% Specificity: 78.05% Accuracy: 91.17% Sensitivity: 99.65%
Ischemic strokes [27]	MRDWI-242 Private areas: Testing (90), Training (90), Validations (62) Extra datasets: ISLES2015	CNN-3D	Precision Lesionwise: 92.67% F1 score Lesion wise: 89.25% DSC: 79.13%
Ischemic strokes [29]	MR-DWIPWI ISLES 2016- 2017	RF-CNN	Comparisons of methods built in Challenge ISLES 2016-2017.
Ischemic strokes [32]	MRI-222 patients	deep CNN	AUC = $0.88 \pm 0.12$
Brain lesions: Brain tumour Ischemic stroke [33]	SPES belong to MICCAI - ISLES: 30 trainings, 20 challenges MRI-multimodalities BRATS 2013: Trainings (30), Leader board (25), Challenges (10)	Restriction based Boltzmann Device for unsupervised dependent features learning, and RF classifiers	SPES Dice scores: $0.75 \pm 0.14$ BRATS 2013 Dice scores: 0.81 ASSD: $2.43 \pm 1.93$
Ischemic strokes [34]	MRI_DWI: 12 subjects	ANN	Prediction correlation Map ( $r = 0.80$ , $p < 0.0001$ )

### III. Datasets of Brain images and Analysis

The primary goal is to evaluate the performance of the developed stroke detection system. This involves assessing its accuracy and effectiveness in distinguishing between

normal and diseased brains. Due to the limited availability and ethical considerations of clinical images, you've opted to use benchmark datasets for evaluation purposes. Benchmark datasets often provide standardized and well-annotated

images that can be used for testing and comparing algorithms. MRI is a common and powerful imaging modality used in medical diagnostics, providing detailed images of the internal structures of the brain. The implementation of the detection mechanism involves using 3D images. 3D images provide a volumetric representation, allowing for a more comprehensive analysis of the brain structures. This can enhance the system's ability to detect strokes accurately. The flexibility in choosing modalities for image registration is highlighted. This includes the selection

of different MRI modalities such as Diffused Weight, Flair, and T1. Image registration is a critical step in aligning images for accurate comparison and analysis. For each modality, you've considered 500 training images and 200 testing images. The dataset images in Figure 2 the sample brain images allows for training the system on a substantial dataset and evaluating its performance on a separate set of images seen during training.

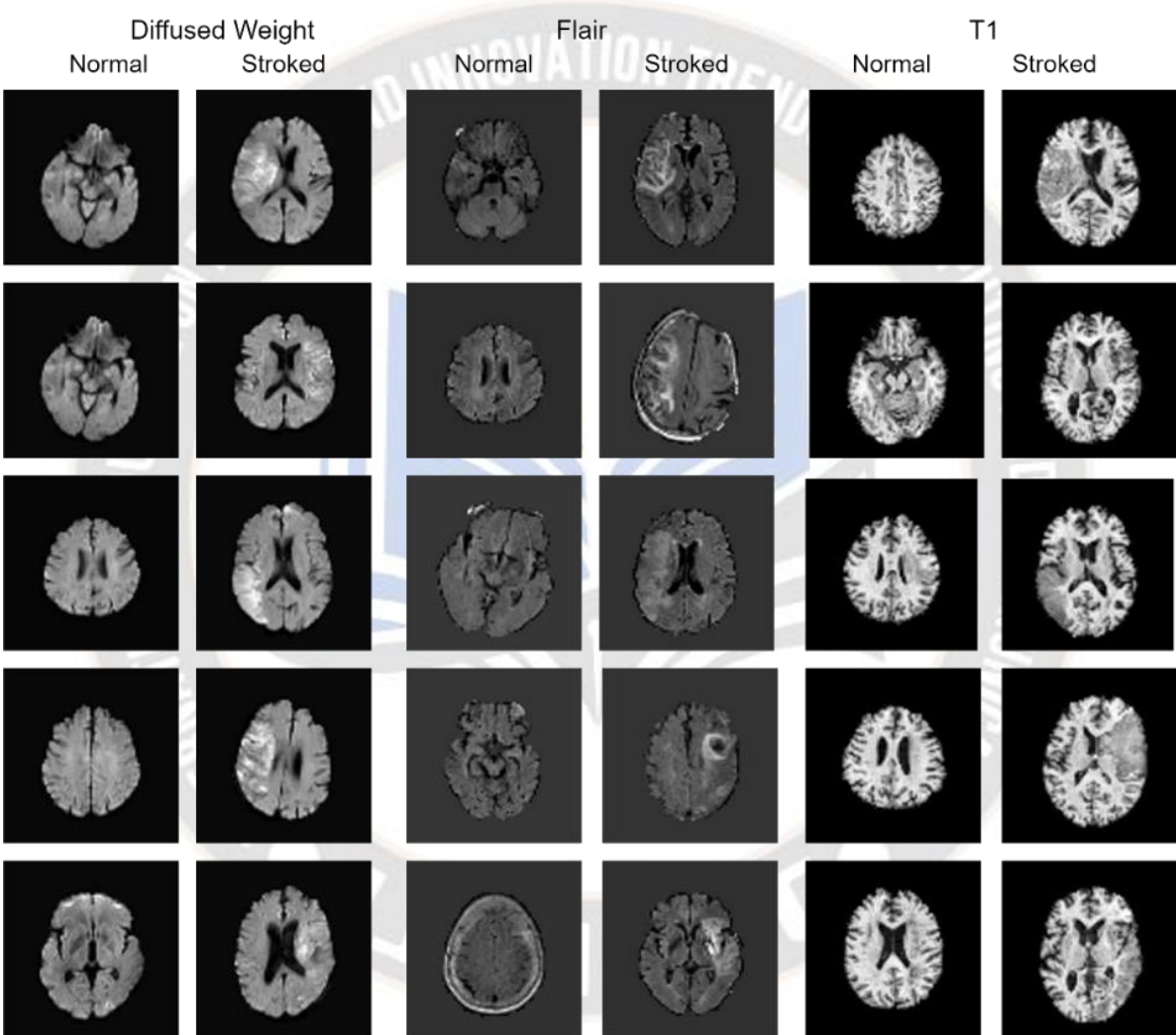


Fig. 2: Brain images utilized in the work

All images of lesion describe the process of precisely labeling lesion images by experienced brain specialists. Their expertise ensures accurate identification and annotation of lesions within the medical images. Labeling tools are software applications designed for marking specific objects or regions of interest within images. The annotation process involves defining bounding boxes around the identified lesions. Information related to the lesions are

saved in an XML file. The XML file not only includes basic image information like channels, width, and height but also contains crucial details about the labeled lesions. This includes information about lesion categories, specifying the type or nature of the lesion, and the coordinates of the bounding boxes, providing precise spatial information. The methodology and analysis conducted on the dataset containing medical reports and images related to ischemic



strokes. The dataset is constructed by randomly selecting reports and images from ischemic stroke medical data. This approach aims to ensure the dataset objectively reflects the comprehensive characteristics of ischemic strokes. Before utilization in research activities, both imaging images and reports

undergo anonymization. Anonymization is a crucial step to protect patient privacy and adhere to ethical considerations. The collected MRI data and reports undergo statistical analysis and visualization using Excel. This step is essential for exploring and understanding the inherent therapeutic information about ischemic strokes present in the dataset. The process of data analysis is segmented based on statistical and tabular approaches. This segmentation helps organize and structure the data, making it easier for storage, retrieval, and further exploration. Five aspects are considered in the analysis of clinical reports and MRI images. These aspects include age, gender, lesion shape, location of lesion, and possible diseases. The tabular approach is used for analysis, implying that data is organized into tables for systematic examination. This can facilitate easier queries and insights into the relationships and patterns present in the dataset. Based on the collected data, the gender proportion analysis reveals that the ratio of male to female patients is approximately 55:45. This suggests that, according to the dataset, males are more likely to suffer from ischemic stroke than females.

The average age of the 500 patients is reported as 65.8 years, with a minimum age of 20 and a maximum age of 84. This provides a snapshot of the overall age range in the dataset.

The quantity of instances in various age groups is determined. Specifically, in Figure 3 it is mentioned that around 85% of the patients are aged above 50. This statistic is crucial for understanding the age distribution and identifying the predominant age range affected by ischemic strokes. The statement suggests that age sections between 50 and 80 may be considered a risk zone, indicating that individuals within this age range are more likely to be affected by ischemic strokes. This observation aligns with the general understanding that stroke risk tends to increase with age.

The analysis of medical diagnosis data related to ischemic stroke patients. Outcome is displayed through Figure 4. The dataset primarily focuses on ischemic strokes, and the analysis concludes that 100% of the cases result in cerebral necrosis. This aligns with the nature of the dataset, emphasizing the prevalence of ischemic strokes. The second most common condition among stroke patients is senile degeneration of the cerebrum, accounting for 79% of cases. Senile degeneration refers to the gradual deterioration of brain tissue, and it is noted as a prevalent chronic condition, particularly in middle and older ages. Cerebral atrophy, a form of weak degeneration of the cerebrum, is identified as the third most common condition. This degenerative change in the brain is noted as a common chronic illness in middle and older ages. Sinusitis, a chronic inflammation of the sinuses, is identified as the third most common condition. Out of 500 stroke patients, 310 patients possess sinusitis, affecting 62% of the stroke patients in the dataset. This high prevalence suggests a notable association between sinusitis and ischemic strokes.

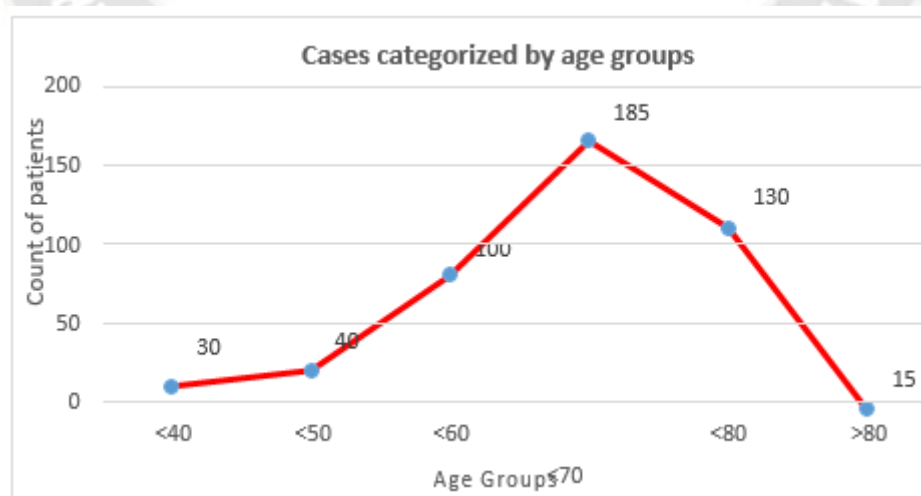


Fig. 3: Cases categorized by age groups.

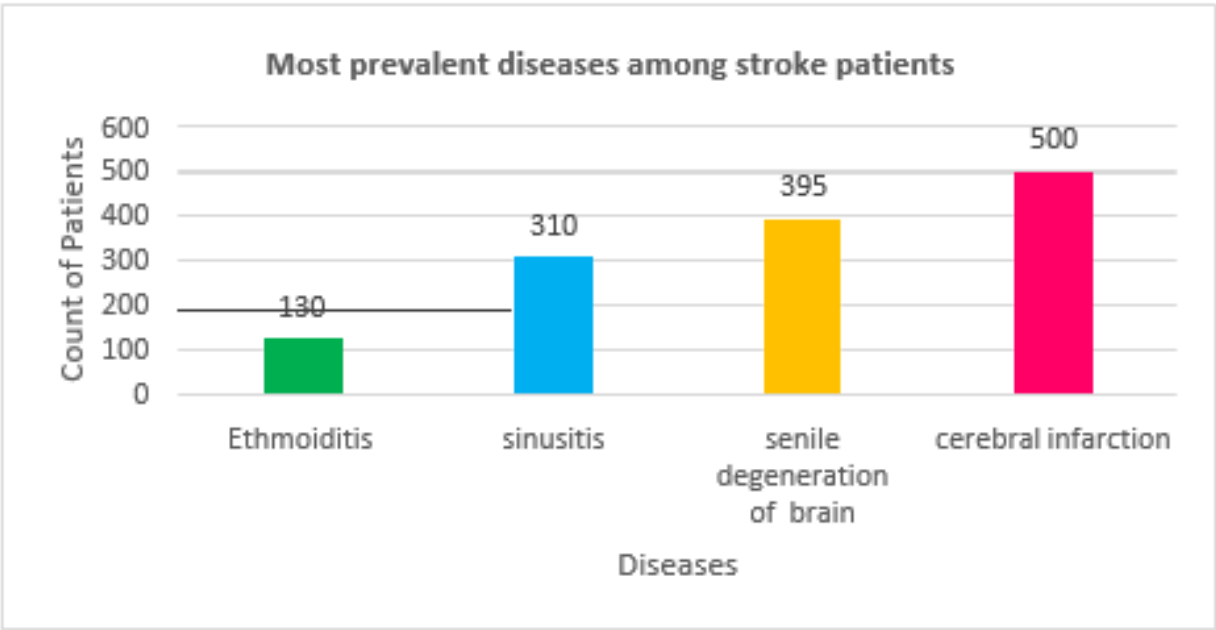


Fig. 4: Most common diseases of stroke patients

The analysis focuses on dissecting the vocabulary used in MRI descriptions, specifically in the context of findings related to lesion locations in stroke patients. The emphasis is on identifying high-frequency areas or locations where lesions are commonly found in stroke patients. This information is crucial for understanding the patterns and prevalence of lesions in different brain regions. The analysis

likely considers not only the location but also the state or characteristics of the lesions. This could include factors such as lesion size, shape, and other relevant features. The results of this data analysis are expected to have implications for the reliability of predicting, diagnosing, and treating ischemic stroke, as displayed in Figure 5.

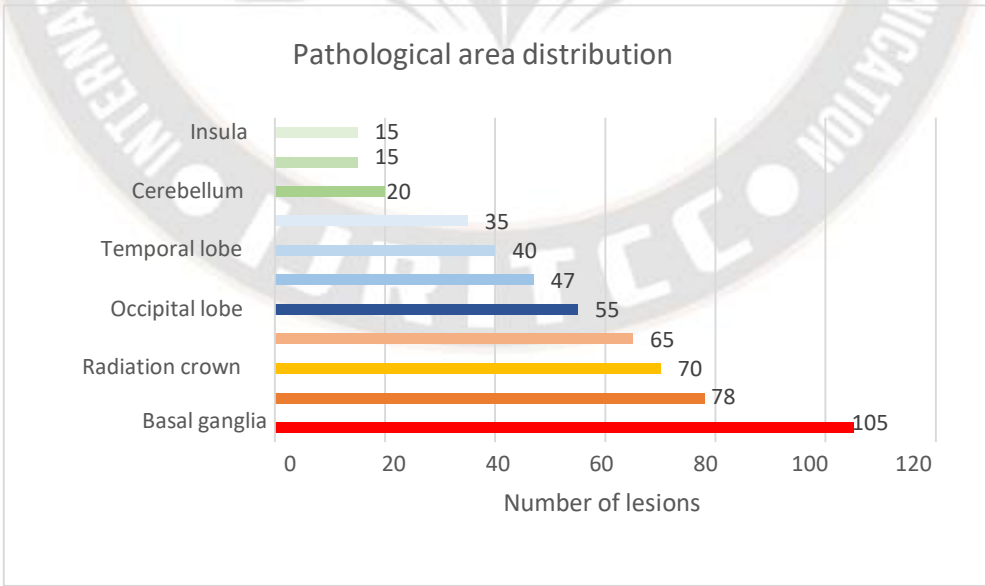


Fig. 5: Statistics of Pathological Area distributions

Figure 5 shows several brain regions among which frontal lobe, basal ganglia, pons, radiation crown, temporal lobe,

parietal lobe, occipital lobe, thalamus, and cerebellar hemispheres can be seen. The analysis indicates that the basal

ganglia had the largest number of injuries, with 105 cases, followed by the frontal lobe with 78 cases. The radiation crown had 70 instances of injuries. A higher number of injuries in a specific brain region may correlate with a higher risk. This perspective is important for understanding the severity

and potential impact of lesions in different areas. Following

the analysis, four areas – the frontal lobe, basal ganglia, pons, radiation crown, temporal lobe, and parietal lobe, and the occipital lobe – are identified as the most common sites of cerebral necrosis. Thalami and other hemispheric parts are also noted as regions that have the opportunity for strokes. Fig 6 exhibits the regions of brain that are in common among the individuals with higher incidence.

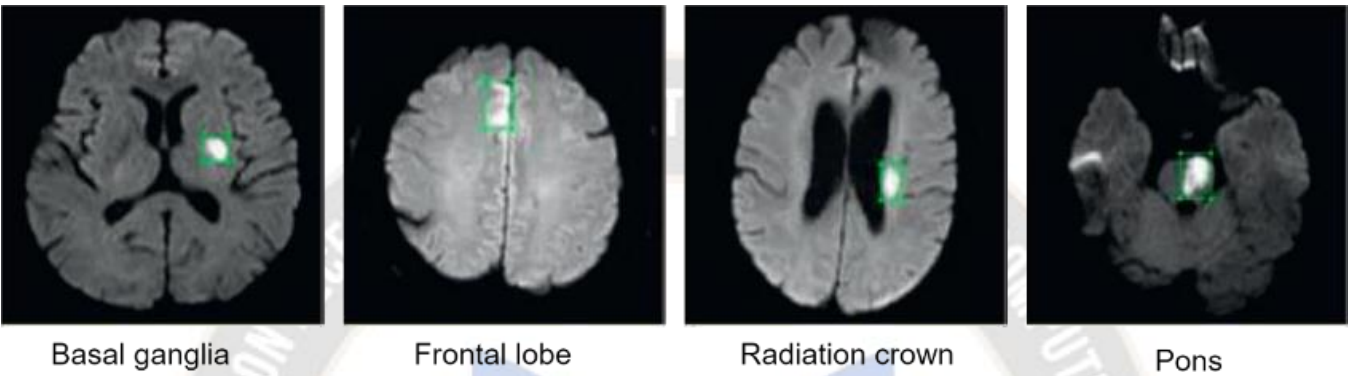


Fig. 6: Regions exhibiting a higher frequency of lesions.

Lesion shape is identified as the 5<sup>th</sup> index in the analysis, suggesting that the shape of the injury region is considered when assessing stroke-related data. It is noted that approximately half of the total lesions have sketchy records. This may indicate a level of subjectivity in the shape descriptions provided by radiologists. The

shape of the injury region, being influenced by radiologists' subjective factors, can lead to different shape descriptions for similar lesions. This subjectivity introduces variability in the assessment and documentation of lesion shapes.

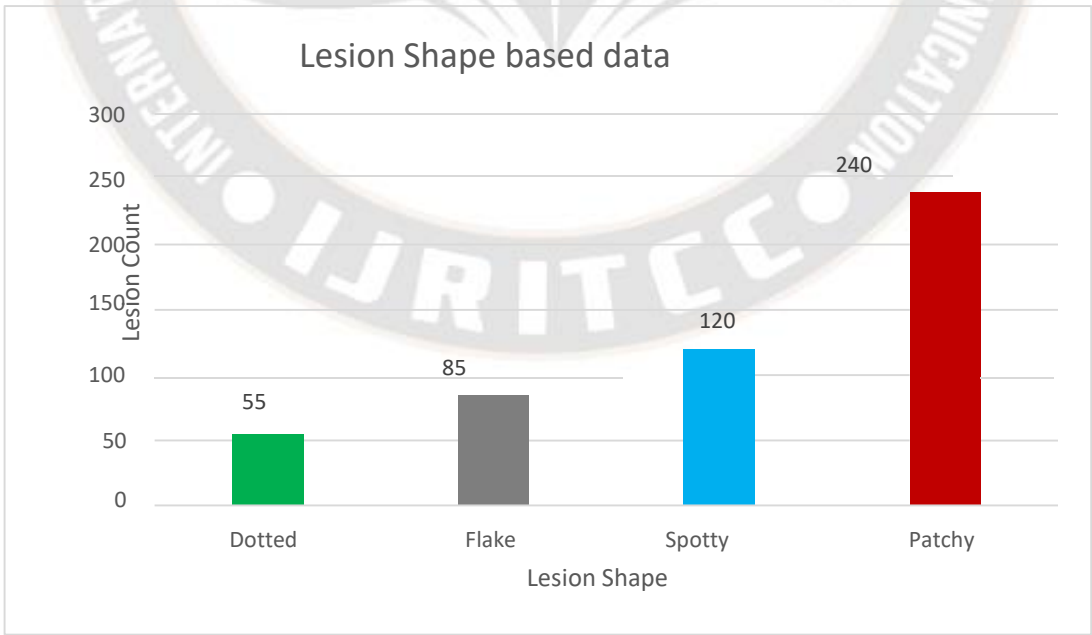


Fig. 7: Facts based on Lesion Shapes



#### IV. Methodological approach

Various schemes are discussed in literature to detect ischemic stroke lesions in brain MRI datasets with improved accuracy. The proposed methodology involves several phases illustrated in Figure 8. (a) Identifying and delineating the boundaries of stroke lesions in the brain. (b) Extracting relevant features from the segmented lesions. (c) Utilizing a deep learning framework to extract intricate features from the data. (d) Employing a classification mechanism to categorize the lesions. SSD-based segmentations and classifications are employed as part of the proposed technique. SSD is a type of object detection algorithm, and its application in this context aims to enhance the accuracy of lesion detection. The deep learning framework is designed to handle multiple tasks, including feature extraction and classification. This involves leveraging the capabilities of neural networks to automatically learn and represent complex patterns within the data. The outlined phases, from segmentation to classification, represent a

comprehensive workflow for analyzing brain MRI datasets and identifying ischemic stroke lesions.

Segmentation is carried out using the VGG-SegNet system, which is composed of the encoder and decoder SSD components in the pipeline. "SoftMax layer" is the last layer of the VGG16 architecture. The encoding and decoding processes involve features as the images are extracted and reconstructed, respectively. The encoding layer of the network provides deep features that are reduced in dimensionality using fully connected layers. Next, the classification process is refined by integrating the combined features that have been assessed through the deep learning classification with deep features. The features incorporated in this method include Local Binary Patterns (LBP) and Grey-level Co-occurrence Matrix (GLCM), which are combined with the existing features to enhance the classifier performance.

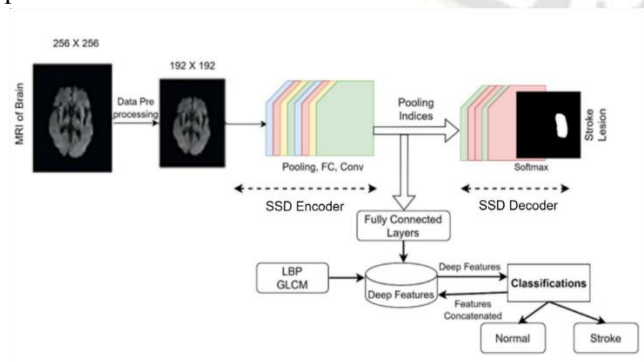


**Fig. 8:** Proposed Architecture of Faster R-CNN

In this study, we utilize three state-of-the-art object

detection networks—SSD (Single Shot Detector), R-CNN (Region-based Convolutional Neural Network), and YOLOv3 (You Only Look Once)—to automatically identify lesions associated with ischemic stroke within collected datasets. The R-CNN approach incorporates either VGG16 or ResNet101 for feature extraction, resulting in the evaluation of a total of four distinct object detection networks.

The R-CNN method follows a two-stage design for lesion detection. Initially, the Region Proposal Network (RPN) generates Regions of Interest (ROIs), which then undergo classification and regression. Leveraging pre-trained weights from VGG16 or ResNet101 models trained on ImageNet for feature extraction initialization enhances the overall effectiveness of the detection process. This comprehensive approach aims to improve lesion detection accuracy and efficiency in ischemic stroke diagnosis.

The YOLOv3 is employed for object detection, utilizing direct regression to determine object location through a one-stage network. The network architecture is based on DarkNet-53, drawing on the residual concept of ResNet to facilitate smoother convergence. Unlike traditional approaches, YOLOv3 utilizes multi-layered feature maps without pooling layers, enhancing the efficiency of the model. We opted for Tiny-Darknet to ensure efficient object detection. YOLOv3 incorporates multiscale predictions like Feature Pyramid Networks (FPN), replacing SoftMax operations with strategic functions to handle prediction scores for classifications. The strategic classifiers operate independently of each other, enabling the model to achieve multicategory predictions efficiently.

In alignment with the principles of R-CNN and YOLOv3, SSD adopts a single-stage network for region generation and leverages information from multi-faceted features. The algorithm utilizes VGG-SegNet for feature extraction, incorporating several convolutional layers and a 3x3 convolution kernel to predict features at different depths and sizes for categorization. The regression values for preselection boxes are computed, and the outcome is determined through network loss. A key distinction of SSD from YOLOv3 lies in the prediction process. In SSD, features are predicted independently from shallow to deep layers without deep fusions. This characteristic differentiates SSD's approach to feature extraction and enhances its capacity for efficient object detection.

In the field of medical research, image-based feature classification is generally accepted as the backbone of designing precision diagnostic tests, as the quality of the test results is directly proportional to the image features utilized. In our experiment, we deploy deep features through pre-trained mechanisms, for example, SSD, ResNet101,

SoftMax for classifications. Deep features we can extract in the encoding stage are used to reduce the number of features by means of fully connected layers in our proposed framework. Among the features are handcrafted features, which include Local Binary Patterns (LBP) [40][41] and Gray-Level Co-occurrence Matrix (GLCM) [42][43][44]. GLCM has demonstrated its own top performance for sure, so it becomes very important. The dimensionality of the feature vector is optimized by a concatenation of features, where both deep and handcraft features are joined at their ends. Finally, the concatenated vector is used for training, testing, and cross-validation of the classifiers' performance. This methodology is aimed at taking advantage of the strong points of both the deep and handcrafted features to ensure that the classifier utilizes both of them in the medical image-based applications.

The second stage of the evaluation process is circumscribed by the type of images the category of classifiers is intended to classify. The proposed work utilizes binary classification

that distinguishes several modalities of brain images as normal or stroked.

SoftMax begins as the default classifier for the task at hand: classification. The process after that consists of distinct classifiers consisting of Decision Tree (DT), Support Vector machines (SVM), K-nearest neighbours (KNN), and Random Forest (RF). We carry out specific evaluation of each classifier using the classifier's success rate as a benchmark. The classifiers' outputs are closely inspected, and the best classifier is identified as the result to prove the framework's overall performance.

Evaluation of the proposed research is done relying on values obtained from the metrics computed from the PT, NT, PF and NF. These values are then used in such metrics that are composed of Accuracy, Sensitivity, Precision, F1-score as well as Negative Predictions Values (NPV) [25][26][27]. This equation to calculate these is mathematically given as:

**Accuracy:** 
$$Accuracy = \frac{PT+NT}{PT+NT+PF+NF}$$

**Sensitivity (Recall or True Positive Rate):** 
$$Sensitivity = \frac{PT}{PT + NF}$$

**Precision (Positive Predictive Value):** 
$$Precision = \frac{PT}{PT + PF}$$

**F1-Score (Harmonic Mean of Precision and Sensitivity):**

$$F1 - score = \frac{2PT}{2PT + PF + NF}$$

**Negatively Predicted Values (NPV):**

$$NPV = \frac{NT}{NT + NF}$$

## V. Results Analysis and Discussions

The experimental section presents the examination about the outcomes of the application of standard machines and MATLAB where the automated lesion detection takes place using the object identification networks of three classes. The dataset is split into the training and testing sets, having 500 images and 200 images accordingly. In the case of Table 2 the results are quantized and presented.

The data suggests that the exactness of lesion detection, which was realized by VGG16, ResNet101, and YOLOv3 networks is comparatively lower than SSD, but it performs better. It follows that the capacities and flexibility of the SSD in detecting such diverse kinds of lesions is superior to those of conventional radiology. The fact that the SSD network can handle all the different types of lesions means that it is a more suitable choice for automated lesion detection than are other networks discussed.

The major intent of the work is designing a deep learning system that is specifically for the segmentation and

classification of MRI images and mainly aimed at the detection of ischemic strokes. The evaluation of the

proposed framework is done separately for the modalities namely Diffuse weight, Flair, and T1 test images, respectively. The process evaluation involves LBPs (Local Binary Patterns) and GLCM (Gray-Level Co-occurrence Matrix) features extraction from the specific weight test pictures.

Figure 9 is composed of 9(a), 9(b), and 9(c) that respectively presents testing image samples and the corresponding LBP patterns for all three modalities 9(a), 9(b), and 9(c) while 9(d), 9(e), and 9(f) display the LBP patterns for Diffuse Weight, Flair, and T1 modal.

For testing samples, afterwards, we will classify each of them individually by applying the Deep Learning techniques. This refers to the process of leveraging the tooled features to classify or tag the images, which is mostly determined by the presence or absence of ischemic stroke signs. The implementation of deep learning methods for the

segmentation phase of the framework guarantees accuracy and improves overall effectiveness as the artificial intelligence will detect and classify ischemic strokes in MRI

images regardless of the modality.



**Fig. 9:** Examining image samples and patterns of Local Binary Patterns for Diffused Weight, Flair, and T1 modalities.

The experimentation results are presented in Table 2, showcasing computed metric values for various schemes applied to different MRI modalities. Deep features are employed using the SoftMax classifier, revealing that the Diffused Weight and Flair modalities outperform the T1 modality. Figure 10 provides a graphical analysis of the results, from 10-a to 10-e illustrating the analysis of accuracy, sensitivity, precision, F1-score, and NPV for the proposed framework with deep features and SoftMax across diffused weight, flair, and T1 modalities.

The analysis shows the advantage of superb accuracy and quality of metric value of SSD over other deep learning architectures. The final step of the SSD test

procedure is to replace the SoftMax classifier with SVM, KNN, DT and RF classifiers as shown in Table 3 and in Fig. 11. Parts 11-a to 11-e focus on the analysis of accuracy, sensitivity, precision, F1-score, and NPV which are the measures used for the proposed model with 3 MRI modalities: diffused weight, flair, and T1. The tests showed that deep features with the KNN approach give more accurate results than any classification techniques. The experiment is extended with the aim of exploring the potential improvements in the ischemic stroke detection and classification in MRI images by combining both deep learnt features and handcrafted ones.

**Table 2:** Assessment of outcomes using deep features in conjunction with SoftMax.

Network Schemes	MRI Modalities	PT	NF	NT	PF	Accuracy	Sensitivity	Precision	F1-Score	NPV
R-CNN_VGG16	Diffused Weight	179	21	273	27	90.40	89.50	86.89	88.40	92.86
	Flair	175	25	275	25	90.00	87.50	87.50	87.50	91.67
	T1	145	55	239	61	76.80	72.50	70.39	71.43	81.29
YOLOv3	Diffused Weight	166	34	276	24	88.40	83.00	87.37	85.13	89.03
	Flair	172	28	270	30	88.40	86.00	85.15	85.57	90.60
	T1	158	42	243	57	80.20	79.00	73.49	76.14	85.26
SDD	Diffused Weight	177	23	279	31	91.20	88.50	85.10	86.76	92.38
	Flair	172	28	282	22	90.80	86.00	88.66	87.31	90.97
	T1	142	58	262	51	80.80	71.00	73.58	72.26	81.88
R-CNN_ResNet101	Diffused Weight	160	40	281	19	88.20	80.00	89.39	84.43	87.53
	Flair	172	28	279	21	90.20	86.00	89.12	87.53	90.88
	T1	135	65	260	40	79.00	62.50	77.14	72.00	80.00



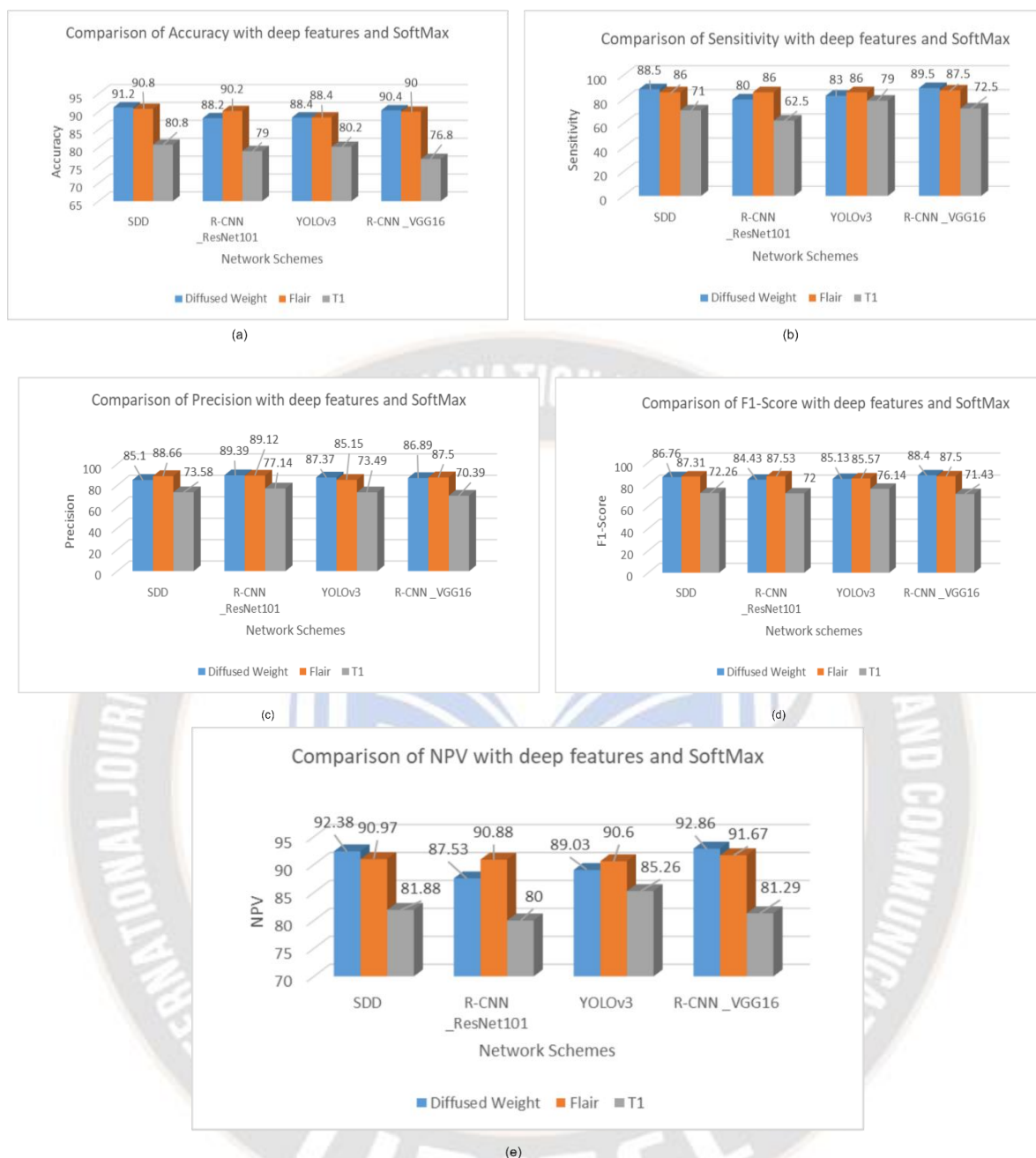


**Fig. 10:** Visual representation of findings with “deep features” and “SoftMax”

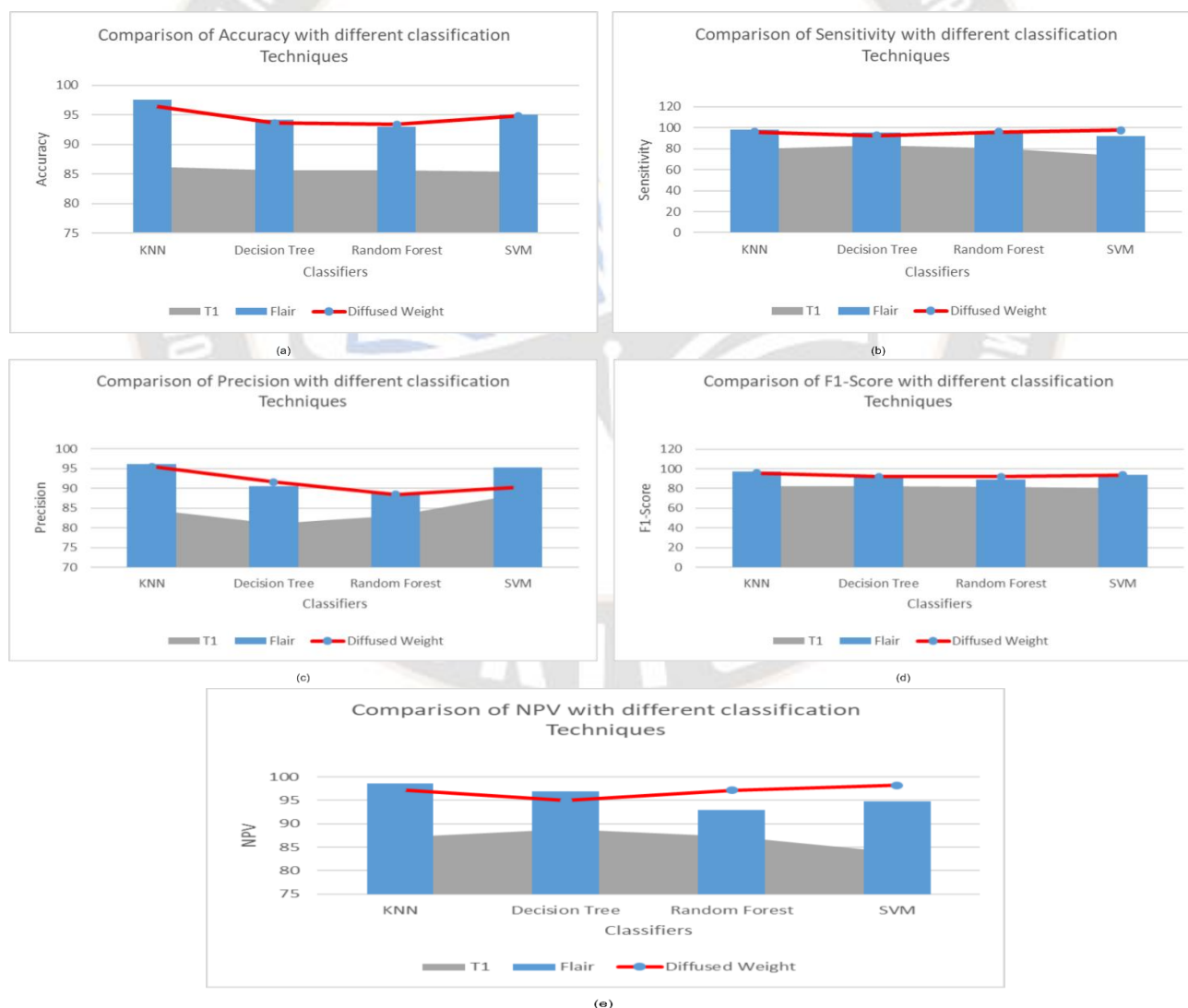
**Table 3:** Analysis of the performance of the proposed Software Design Document (SDD) using different classification techniques.

Network Schemes	MRI Modalities	PT	NF	NT	PF	Accuracy	Sensitivity	Precision	F1-Score	NPV
SVM	Diffused Weight	195	05	279	21	94.80	97.50	90.28	93.75	98.24
	Flair	184	16	291	09	95.00	92.00	95.34	93.64	94.79
	T1	146	54	281	19	85.40	73.00	88.48	80.00	83.88
KNN	Diffused Weight	192	08	291	09	96.60	96.00	95.52	95.76	97.32
	Flair	196	04	292	08	97.60	98.00	96.08	97.03	98.65
	T1	160	40	271	29	86.20	80.00	84.66	82.26	87.14
RandomForest	Diffused Weight	192	08	275	25	93.40	96.00	88.48	92.09	97.17
	Flair	189	21	276	24	93.00	94.50	88.73	89.36	92.93
	T1	161	39	267	33	85.60	80.50	82.99	81.73	87.25
Decision Tree	Diffused Weight	185	15	283	17	93.60	92.50	91.58	92.04	94.97

Flair	191	09	280	20	94.20	95.50	90.52	92.94	96.89
T1	167	33	261	39	85.60	83.50	81.07	82.27	88.78

**Table 4:** Analysis of classifiers applied to the proposed Software Design Document using concatenated features.

Network Schemes	MRI Modalities	PT	NF	NT	PF	Accuracy	Sensitivity	Precision	F1-Score	NPV
SVM	Diffused Weight	196	04	297	03	98.60	98.00	98.49	98.25	98.67
	Flair	197	03	291	09	97.60	98.50	95.63	97.04	98.97
	T1	184	16	288	12	94.40	92.00	93.88	92.93	94.74
KNN	Diffused Weight	188	12	288	12	95.20	94.00	94.00	94.00	96.00
	Flair	192	08	292	08	96.80	96.00	96.00	96.00	97.33
	T1	172	28	278	22	90.00	86.00	88.66	87.31	90.85
RandomForest	Diffused Weight	191	09	279	21	94.00	95.50	90.09	92.72	96.88
	Flair	192	08	276	24	93.60	96.00	88.89	92.31	97.18
	T1	169	31	275	25	88.80	84.50	87.11	85.79	89.87
Decision Tree	Diffused Weight	194	06	283	17	94.40	97.00	91.94	94.40	97.92
	Flair	193	07	286	14	95.80	96.50	93.24	94.84	97.61
	T1	167	33	264	34	86.20	83.50	83.08	83.29	88.89

**Fig. 11:** Analysis of the results of the Software Design Document (SDD) employing different classifiers.



**Fig. 12:** Analysis of the results from Software Design Document (SDD) utilizing different classifiers with concatenated features.

The experimental results, employing concatenated features, are outlined in Table 4. Evaluation metrics highlight the superior performance of the Diffused Weight image set, affirming that SVM-based classification outperforms the other three techniques employed in the experiments. Figure 12 offers a visual analysis, where sub-figures 12-a to 12-e depict the assessment of accuracy, sensitivity, precision, F1-score, and NPV for the proposed framework, utilizing classifiers with concatenated features across MRI modalities Diffused Weight, Flair, and T1.

**Comparisons with existing methodologies:** In Table 5 outlines the performance of the proposed framework across Diffused Weight, Flair, and T1 modalities in MRI, showcasing superior accuracy values when tested with different classifiers. To offer context and validate the efficacy of the proposed framework, a comparative analysis is conducted with the works of fellow researchers. The table juxtaposes the highest performance attained by the proposed framework with accuracy data collected from other researchers in the field. This comparison is presented in tabular form within Table 5.



Moreover, Figure 13 presents a visual analysis of the outcomes. The sub-figures in Figure 13 juxtapose the efficacy of the proposed framework with that of previous studies concerning Diffused Weight, Flair, and T1 MRI modalities. The graphical depiction of the inquiry demonstrates that the proposed framework surpasses existing works, demonstrating notably superior performance

in terms of accuracy. This comparative assessment accentuates the progress and contributions of the proposed framework in the field of MRI image analysis, specifically in the context of detecting and classifying ischemic strokes.

Table 4: Comparing existing works with framework proposed.

Methodology	Accuracy attained
Anbumozhi [11]	98.8%
Subudhi <i>et al.</i> [30]	93.4%
Melingi [49]	97.8%
Qiu [2]	95%
Proposed Framework (Diffused Weight)	98.60%
Venkatesan [50]	98.17%
Nazari-Farsani <i>et al.</i> [17]	73%
Proposed Framework (T1)	94.40%
Kumar [48]	98.14%
Proposed Framework (Flair)	97.60%

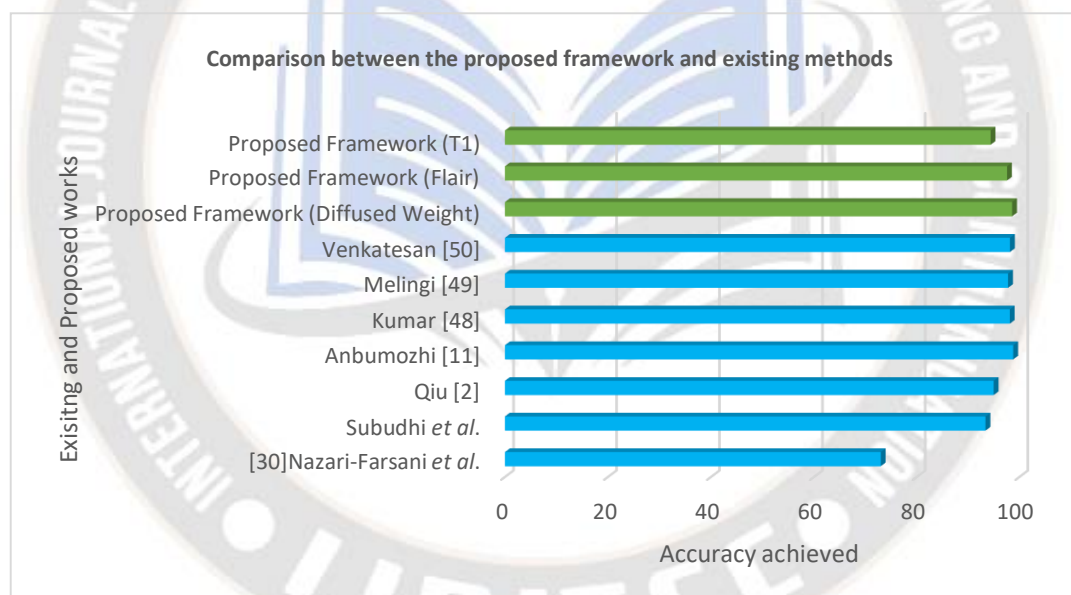


Fig. 13: Comparison between the proposed framework and current methodologies

## VI. Conclusion

The proposed framework initially utilized the SSD technique and executed VGG-SegNet mining, achieving promising results across different modalities of MRI such as Diffused Weight, Flair, and T1.

Subsequently, classification operations were applied, considering a few deep learning mechanisms. The results of SSD demonstrated superior performance compared to other techniques in the context of the tasks. The SSD performance was further validated using deep and concatenated features,

employing SVM, KNN, RF, and DT schemes. The outcomes confirmed that KNN achieved an accuracy of classification of 97.60% for deep features, while SVM recorded the maximum accuracy of classification at 98.60% for concatenated features. This validation showcases the effectiveness of the SSD technique in combination with various classification schemes for accurate detection and classification of ischemic strokes in MRI images.

In future research works, the proposed framework aims to explore a greater number of network schemes and incorporate various deep learning mechanisms. This expansion could

lead to further advancements and improvements in the framework's capability to handle a diverse range of MRI modalities and enhance its performance in detecting and classifying medical conditions, such as ischemic strokes.

## REFERENCES

- [1] Pan, Jiawei & Wu, Guoqing & Yu, Jinhua & Geng, Daoying & Zhang, Jun & Wang, Yuanyuan, "Detecting the Early Infarct Core on Non-Contrast CT Images with a Deep Learning Residual Network", *Journal of Stroke and Cerebrovascular Diseases*. 2021, 30, 105752, doi: 10.1016/j.jstrokecerebrovasdis.2021.105752.
- [2] Qiu W, Kuang H, Teleg E, Ospel JM, Sohn SI, Almekhlafi M, Goyal M, Hill MD, Demchuk AM, Menon BK, "Machine Learning for Detecting Early Infarction in Acute Stroke with Non-Contrast-enhanced CT", *Radiology*, 2020, 294(3):638-644, doi: 10.1148/radiol.2020191193.
- [3] Liew, Sook-Lei & Juliano, Julia & Banks, Nick & Sondag et al, "A large, open-source dataset of stroke anatomical brain images and manual lesion segmentations", *Scientific Data*, 2018,5,180011, doi:10.1038/sdata.2018.11.
- [4] Campbell BCV, De Silva DA, Macleod MR, Coutts SB, Schwamm LH, Davis SM, Donnan G, "Ischaemic stroke", *Nat Rev Dis Primers*, 2019, 5(1):70, doi: 10.1038/s41572-019-0118-8.
- [5] M. Yousefian, A. Amani, H. Seyedarabi and M. Farhoudi, "A comparison study of automated approaches for brain lesions segmentation in ischemic stroke", 28th Iranian Conference on Electrical Engineering (ICEE), 2020, pp. 1-7, doi: 10.1109/ICEE50131.2020.9260774.
- [6] Román LS, Menon BK, Blasco J, Hernández-Pérez M, Dávalos A, Majoie CBLM et al., "Imaging features and safety and efficacy of endovascular stroke treatment: a meta-analysis of individual patient-level data", *Lancet Neurol*, 2018, 895-904, doi: 10.1016/S1474-4422(18)30242-4.
- [7] Wilson AT, Dey S, Evans JW, et al., "Minds treating brains: understanding the interpretation of non-contrast CT ASPECTS in acute ischemic stroke", *Expert Review of Cardiovascular Therapy*, 2018, 16(2):143-153, doi: 10.1080/14779072.2018.1421069.
- [8] Lundervold AS, Lundervold A, "An overview of deep learning in medical imaging focusing on MRI", *Z Med Phys*, 2019, 29(2):102-127, doi: 10.1016/j.zemedi.2018.11.002.
- [9] Raghavendra U, Acharya UR, Adeli H, "Artificial Intelligence Techniques for Automated Diagnosis of Neurological Disorders", *Eur Neurol*, 2019, 82(1-3):41-64, doi: 10.1159/000504292.
- [10] Leite M, Rittner L, Appenzeller S, Ruocco HH, Lotufo R, "Etiology-based classification of brain white matter hyperintensity on magnetic resonance imaging", *J Med Imaging (Bellingham)*, 2015, 2(1):014002, doi: 10.1117/1.JMI.2.1.014002.
- [11] Selladurai Anbumozhi, "Computer aided detection and diagnosis methodology for brain stroke using adaptive neuro fuzzy inference system classifier", *Int. J. Imaging Systems and Technology*, 2019, 30, 196-202, doi:10.1002/ima.22380.
- [12] Acharya, U Rajendra & Meiburger, Kristen & Faust, Oliver & Koh et al., "Automatic detection of ischemic stroke using higher order spectra features in brain MRI images", *Cognitive Systems Research*, 58, doi: 10.1016/j.cogsys.2019.05.005.
- [13] Sabut, Sukanta & Subudhi, Asit & Biswal, Pradyut & Sahoo, Santanu, "Segmentation and classification of ischemic stroke using optimized features in brain MRI", *Biomedical Engineering*, 30, doi: 10.4015/S1016237218500114.
- [14] Ho KC, Speier W, Zhang H, Scalzo F, El-Saden S, Arnold CW, "A Machine Learning Approach for Classifying Ischemic Stroke Onset Time from Imaging", *IEEE Trans Med Imaging*, 2019, 38(7):1666-1676. doi: 10.1109/TMI.2019.2901445.
- [15] Castillo, Darwin, Vasudevan Lakshmi Narayanan, and María J. Rodríguez-Álvarez, "MR Images, Brain Lesions, and Deep Learning", *Applied Sciences*, 2021, 11, no. 4: 1675. Doi:10.3390/app11041675.
- [16] Bhandary, Abhir & G, Ananth & Basthikodi, Mustafa & M, Chaitra, "Early Diagnosis of Lung Cancer Using Computer Aided Detection via Lung Segmentation Approach". *International Journal of Engineering Trends and Technology*, 2021, 69. 85-93, doi:10.14445/22315381/IJETT-V69I5P213.
- [17] Nazari-Farsani S, Nyman M, Karjalainen T, Bucci M, Isojärvi J, Nummenmaa L, "Automated segmentation of acute stroke lesions using a data-driven anomaly detection on diffusion weighted MRI", *J Neurosci Methods*, 2020,333:108575. doi: 10.1016/j.jneumeth.2019.108575.
- [18] Maier O, Schröder C, Forkert ND, Martinetz T, Handels H, "Classifiers for Ischemic Stroke Lesion Segmentation: A Comparison Study", *PLoS One*, 2015, 10(12):e0145118. doi: 10.1371/journal.pone.0145118.
- [19] Swinburne, Nathaniel & Holodny, Andrei, *Neurological Diseases: Opportunities, Applications and Risks*, 2019, 10.1007/978-3-319-94878-2\_15.

- [20]. Sarmiento RM, Vasconcelos FFX, Filho PPR, Wu W, de Albuquerque VHC, "Automatic Neuroimage Processing and Analysis in Stroke-A Systematic Review", *IEEE Rev Biomed Eng*, 2020;13:130-155. doi: 10.1109/RBME.2019.2934500.
- [21]. Amin J, Sharif M, Yasmin M, Saba T, Anjum MA, Fernandes SL, "A New Approach for Brain Tumor Segmentation and Classification Based on Score Level Fusion Using Transfer Learning", *J Med Syst.*, 2019, 43(11):326, doi: 10.1007/s10916-019-1453-8.
- [22] Hussain, S.; Anwar, S.M.; Majid, M, "Segmentation of glioma tumours in brain using deep convolutional neural network", *Neurocomputing*, 2017, 282, 248–261, doi: 10.1016/j.neucom.2017.12.032.
- [23] Nadeem, M.W.; Ghamdi, M.A.A.; Hussain, M.; Khan, M.A.; Khan, K.M.; Almotiri, S.H.; Butt, S. A, "Brain Tumor Analysis Empowered with Deep Learning: A Review, Taxonomy, and Future Challenges", *Brain Sci.* 2020, 10, 118, doi:10.3390/brainsci10020118.
- [24] Huang S, Shen Q, Duong TQ, "Quantitative prediction of acute ischemic tissue fate using support vector machine", *Brain Res.*, 2011, 1405:77-84. doi: 10.1016/j.brainres.2011.05.066.
- [25] Rajinikanth V, Thanaraj K.P, Satapathy S.C, Fernandes S.L, Dey N, "Shannon's Entropy and Watershed Algorithm Based Technique to Inspect Ischemic Stroke Wound", In *Proceedings of the Smart Modelling for Engineering Systems*; Springer International Publishing: USA, 2019, 23–31.
- [26] Chen L, Bentley P, Rueckert D, "Fully automatic acute ischemic lesion segmentation in DWI using convolutional neural networks", *Neuroimage Clin.*, 2017, 15:633-643. doi: 10.1016/j.nicl.2017.06.016.
- [27]. Zhang R, Zhao L, Lou W, Abrigo JM, Mok VCT, Chu WCW, Wang D, Shi L, "Automatic Segmentation of Acute Ischemic Stroke from DWI Using 3-D Fully Convolutional DenseNets", *IEEE Trans Med Imaging*. 2018, 37(9):2149-2160. doi: 10.1109/TMI.2018.2821244.
- [28] Subudhi, Asit Kumar et al., "Automated segmentation and classification of brain stroke using expectation-maximization and random forest classifier", *Biocybernetics and Biomedical Engineering*, 2020, 40: 277-289, doi: 10.1016/J.BBE.2019.04.004.
- [29]. Winzeck S, Hakim A, McKinley R, Pinto JAADSR, Alves V, Silva C et al., "ISLES 2016 and 2017-Benchmarking Ischemic Stroke Lesion Outcome Prediction Based on Multispectral MRI", *Front Neurol.*, 2018, 9:679, doi: 10.3389/fneur.2018.00679.
- [30] Kamnitsas K, Ledig C, Newcombe VFJ et al., "Efficient multi-scale 3D CNN with fully connected CRF for accurate brain lesion segmentation", *Med Image Anal.* 2017, 36:61-78. doi: 10.1016/j.media.2016.10.004.
- [31] V. Rajinikanth, Suresh Chandra Satapathy, "Segmentation of Ischemic Stroke Lesion in Brain MRI Based on Social Group Optimization and Fuzzy-Tsallis Entropy", *Arabian Journal for Science and Engineering*, 2018, 43, 4365–4378, doi: 10.1007/s13369-017-3053-6.
- [32] Nielsen A, Hansen MB, Tietze A, Mouridsen K, "Prediction of Tissue Outcome and Assessment of Treatment Effect in Acute Ischemic Stroke Using Deep Learning", *Stroke*, 2018, 49(6):1394-1401. doi: 10.1161/STROKEAHA.117.019740.
- [33] Pereira S, Meier R, McKinley R, Wiest R, Alves V, Silva CA, Reyes M, "Enhancing interpretability of automatically extracted machine learning features: application to a RBM-Random Forest system on brain lesion segmentation", *Med Image Anal.*, 2018, 44:228-244. doi: 10.1016/j.media.2017.12.009.
- [34] Bagher-Ebadian H, Jafari-Khouzani K, Mitsias PD, Lu M, Soltanian-Zadeh H, Chopp M, Ewing JR, "Predicting final extent of ischemic infarction using artificial neural network analysis of multi-parametric MRI in patients with stroke", *PLoS One*, 2011, 6(8):e22626. doi: 10.1371/journal.pone.0022626.
- [35] Karthik R, Menaka R, Hariharan M, Won D, "Ischemic Lesion Segmentation using Ensemble of Multi-Scale Region Aligned CNN", *Comput Methods Programs Biomed.*, 2021, 200:105831. doi: 10.1016/j.cmpb.2020.105831.
- [36] Liu L, Kurgan L, Wu FX, Wang J., "Attention convolutional neural network for accurate segmentation and quantification of lesions in ischemic stroke disease", *Med Image Anal.*, 2020, 65:101791. doi: 10.1016/j.media.2020.101791.
- [37] Lin, David & Rajinikanth, Venkatesan & Lin, Hong, "Hybrid Image Processing-Based Examination of 2D Brain MRI Slices to Detect Brain Tumor/Stroke Section: A Study" 2020, doi: 10.1007/978-981-15-6141-2\_2.
- [38]. Yushkevich PA, Pashchinskiy A, Oguz I, Mohan S, Schmitt JE, Stein JM et al., "User-Guided Segmentation of Multi-modality Medical Imaging Datasets with ITK-SNAP", *Neuroinformatics*, 2019, 17(1):83-102. doi: 10.1007/s12021-018-9385-x.
- [39]. Yushkevich PA, Gerig G, "ITK-SNAP: An Interactive Medical Image Segmentation Tool to Meet the Need for Expert-Guided Segmentation of Complex Medical Images", *IEEE Pulse*, 2017, 8(4):54-57. doi: 10.1109/MPUL.2017.2701493.



- [40]. Suh, SungMin & Park, Yongeun & Ko, KyoungMin & Yang, SeongMin & Ahn, Jaehyeong & Shin, Jae-Ki & Kim, SungHwan. "Weighted Mask R-CNN for Improving Adjacent Boundary Segmentation", *Journal of Sensors*, 2021, 1-8, doi: 10.1155/2021/8872947.
- [41]. Gudigar, Anjan & U, Raghavendra & devasia, Tom & Nayak, Krishnananda & Danish, Sheik & Kamath et al., "Global weighted LBP based entropy features for the assessment of pulmonary hypertension", *Pattern Recognition Letters*, 2019, 125, doi: 10.1016/j.patrec.2019.03.027.
- [42]. Ahuja, Sakshi et al., "Deep transfer learning-based automated detection of COVID-19 from lung CT scan slices", *Applied intelligence (Dordrecht, Netherlands)*, 2020, 1-15. 21, doi:10.1007/s10489-020-01826-w.
- [43]. Dhiman, Gaurav & Garg, Meenakshi, "A Novel Content Based Image Retrieval Approach for Classification using GLCM Features and Texture Fused LBP Variants", *Neural Computing and Applications*, 2021, 33. doi:10.1007/s00521-020-05017-z.
- [44]. Xing, Z., Jia, H, "An improved thermal exchange optimization based GLCM for multi-level image segmentation", *Multimed Tools Appl*, 2020, 79, 12007–12040, doi:10.1007/s11042-019-08566-1.
- [45]. Dey, Nilanjan & Zhang, Yu-Dong & Rajinikanth, Venkatesan & Ramamurthy, Dr. Pugalenth & Raja, N, "Customized VGG19 Architecture for Pneumonia Detection in Chest X-Rays", *Pattern Recognition Letters*, 2021, 143, doi: 10.1016/j.patrec.2020.12.010.
- [46]. Kassem, Mohamed & Hosny, Khalid & Damasevicius, Robertas & Eltoukhy, Mohamed Meselhy, "Machine Learning and Deep Learning Methods for Skin Lesion Classification and Diagnosis: A Systematic Review", *Diagnostics*, 2021, 11, 1390, doi:10.3390/diagnostics11081390.
- [47]. Priya, S & Rani, Arockia & Subathra, P. & Mohammed, Mazin & Damasevicius, Robertas & Ubendran, Neha, "Local Pattern Transformation Based Feature Extraction for Recognition of Parkinson's Disease Based on Gait Signal", *Diagnostics*, 2021, 11, 1395, doi:10.3390/diagnostics11081395.
- [48]. Kumar A, Upadhyay N, Ghosal P, Chowdhury T, Das D, Mukherjee A, Nandi D, "CSNet: A new DeepNet framework for ischemic stroke lesion segmentation", *Comput Methods Programs Biomed*, 2020, 193:105524. doi: 10.1016/j.cmpb.2020.105524.
- [49]. Melingi, Sunil & Vivekanand, Vijayalakshmi, "A Crossbred Approach for Effective Brain Stroke Lesion Segmentation", *International Journal of Intelligent Engineering and Systems*, 2018, 11, 286-295, doi:10.22266/ijies2018.0228.30.
- [50] Venkatesan Rajinikanth, Shabnam Mohamed Aslam, Seifedine Kadry, "Deep Learning Framework to Detect Ischemic Stroke Lesion in Brain MRI Slices of Flair/DW/T1 Modalities", *Symmetry*, 2021, 13, 2080, doi:10.3390/sym13112080.